Fatigue fracture behaviour of PEEK: 2. Effects of thickness and temperature

M. Brillhart and J. Botsis*
Department of Civil Engineering, Mechanics and Metallurgy (m/c 246), University of Illinois at Chicago, Chicago, IL 60680, USA
(Received 30 September 1991; revised 14 February 1992; accepted 21 March 1992)

Experimental results on the effects of specimen thickness and environmental temperatures on fatigue fracture behaviour of poly(ether ether ketone) (PEEK) are reported. Low cycle fatigue experiments are conducted on injection moulded single-edge notched specimens of 1.57, 2.70 and 5.42 mm in thickness at ambient temperatures, and on specimens 2.70 mm thick at environmental temperatures of 39, 50, 63, 75 and 100°C. In all the thickness experiments and in the experiments with temperatures of 39 and 50°C, the crack tip profile is initially round. At long crack lengths the crack tip profile changes to a triangular shape. When the test temperature is 63, 75 and 100°C, the crack tip remains round throughout the fracture process. The crack tip angle is primarily dependent upon the test temperature. Examinations of the fracture surfaces and transverse sections indicate that in the thickest specimen, relatively rough fracture surfaces are observed and a few discontinuities (crazes or cracks) underneath the main crack path. Thus, crack propagates in a 'brittle' manner. In all other experiments both 'brittle' and 'ductile' modes of fracture are observed. The point of transition from 'brittle' to 'ductile' fracture is dependent upon the specimen thickness and test temperature. Fatigue striations are seen throughout the fracture surfaces. Correlation of the striations and the number of cycles indicates a one-cycle crack growth mode. Hysteretic losses during fatigue crack growth are negligible until a few cycles prior to unstable fracture. Crack opening displacements are independent of the specimen thickness and increase with rise in temperature. When crack growth rates are correlated with the elastic energy release rate, they are independent of specimen thickness and increase with increase in temperature.

(Keywords: poly(ether ether ketone); fatigue; thickness; temperature; brittle–ductile fracture)

INTRODUCTION

In part 1 of this series of papers the effects of variations in load level on fatigue fracture in poly(ether ether ketone) (PEEK) are reported[1]. These studies indicate both a 'brittle' and a 'ductile' mode of fracture during slow crack propagation. This is assessed by comparing experimentally measured energy release rates and crack opening displacements with the predictions of the linear elastic fracture mechanics and by mechanistic investigations of transverse sections of fractured specimens. The crack length at which the transition from 'brittle' to 'ductile' fracture occurs is dependent upon the load level.

Although these studies provide a valuable insight into the material's behaviour, investigations reported in the literature demonstrate that other factors influence fatigue fracture behaviour in numerous thermoplastics[2]. Among these are specimen geometry, processing conditions, temperature and corrosion.

PEEK is a high temperature thermoplastic which possesses excellent physical and mechanical characteristics. However, it is a relatively new material. Thus, additional studies are needed in order to obtain a greater insight into the material's response to service conditions and so assess its potential applications. The scope of this second paper is aimed at characterizing the mechanisms involved during low cycle fatigue under various environmental temperatures and specimen thicknesses. Essential emphasis is given to the crack tip morphology, the extent of specimen thinning around the crack tip, and crack growth kinetics on injection moulded single-edge notched specimens.

EXPERIMENTAL

Specimen preparation

Injection moulded plaques of semicrystalline PEEK 450G with thicknesses of 6.0, 3.2 and 2.0 mm were provided by ICI (Exton, PA, USA). The surfaces of these plaques were hand sanded or ground in order to remove a layer of amorphous material formed during processing[3]. The depth of grinding or hand sanding was approximately 0.25 mm from each side. Single-edge notched specimens of 80 mm in gauge length and 20 mm in width were cut from these plaques. A V-shaped notch 1 mm deep was milled in the middle of the edge of each specimen. To remove any moisture that the material may have absorbed during specimen preparation the specimens were finally heated in an oven at 140°C for approximately 3 h and then allowed to cool slowly in the oven to room temperature.

Methods

In these studies the effects of specimen thickness and environmental temperature on fatigue crack propagation

*To whom correspondence should be addressed

0032-3861/92/245225-08
© 1992 Butterworth-Heinemann Ltd.

were investigated. Thus, two sets of experiments were conducted. The first set involved experiments on specimens with thicknesses, $t = 5.42$, 2.70 and 1.57 mm. They were performed on a dual actuator servohydraulic MTS system in a laboratory atmosphere. In the second set, five environmental temperatures were investigated, $T = 39$, 50, 63, 75 and 100°C, with a constant specimen thickness of 2.70 mm in each experiment. The latter set of experiments was conducted on a dual actuator Instron testing system equipped with an environmental chamber. To assure a uniform specimen temperature, the specimens were placed in the chamber 1 h prior to fatiguing. By preheating all specimens for an equal amount of time the effect of exposure time to elevated temperatures was equivalent for all specimens. Although five temperature experiments were conducted, only the results of experiments with $T = 50$, 75 and 100°C are reported in this paper. The analysis of crack growth for all five temperature experiments will be presented in a future paper.

All experiments were load controlled with a sinusoidal waveform function and frequency of 0.9 Hz. The maximum (σ_{max}) and minimum (σ_{min}) stresses of the fatigue cycle were held constant at 55.15 MPa and 0 MPa, respectively. These stresses and frequency corresponded[4] to a load ratio of $R = 0$ and an approximate stress rate of 99.27 MPa s^{-1}.

The stress intensity factor was computed from:

$$K_1 = \sigma_{max}(\pi l)^{1/2} f(l/B)$$

where l is the crack length, B is the specimen width and $f(l/B)$ is a correction factor appropriate to the specimen geometry[5]:

$$f(l/B) = \left(\frac{2B}{\pi l}\tan\frac{\pi l}{2B}\right)^{1/2} \times \frac{0.752 + 2.02(l/B) + 0.37\left(1 - \sin\frac{\pi l}{2B}\right)^3}{\cos\frac{\pi l}{2B}}$$

The elastic energy release rate was calculated as:

$$G_1 = \kappa K_1^2/E \qquad (1)$$

where $\kappa = (1 - \nu^2)$ for plane strain and $\kappa = 1$ for plane stress, ν is Poisson's ratio and E is the Young's modulus of the material. It is reported in ref. 3 that the degree of crystallinity of injection moulded PEEK 450G is 23%. For this degree of crystallinity the Poisson's ratio was taken as 0.30, the yield stress[6] σ_y as 91 MPa and Young's modulus[7] as 3.00 GPa.

Since σ_{max} is not small when compared to σ_y, crack tip opening displacements were approximated by[8]:

$$\delta = \frac{K_1^2}{E\sigma_y}\left(1 + \frac{\pi^2}{24}\frac{\sigma_{max}^2}{\sigma_y^2}\right) \qquad (2)$$

Crack opening profiles and crack growth kinetics were recorded on a Hamamatsu video system attached to a Questar long range travelling microscope. All fracture surfaces were examined under a Zeiss universal microscope and a Jeol scanning electron microscope. Observations of the extent of thinning were performed on cross sections normal to the crack path which were prepared according to standard metallographic grinding and polishing techniques[9]. In the temperature studies, load displacement curves were taken on an Instron plotter and in the thickness studies curves were recorded with the use of a Yokagwa plotter.

RESULTS AND DISCUSSION

Thickness effects on crack propagation mechanisms

Typical morphologies of the crack tip are shown in *Figure 1*. Within the resolution of the observations, the crack tip profile is initially round in all three specimen thicknesses investigated. As the crack becomes longer the crack tip shape becomes triangular with a crack tip angle of about 90°. This angle remains fairly constant until a few cycles prior to unstable fracture. The parts of crack surfaces which are formed during the loading portion of each cycle do not belong on the planes of the crack until the next fatigue cycle. Within this time relaxation occurs, which leads to partial contraction of the new surfaces.

Analysis of the hysteresis loops for the thinner specimen reveals that the area of the loop is insignificant during the early stages of fatigue crack propagation. However, an increase in the hysteresis loop area is observed a few cycles prior to fast fracture. This increase in area is attributed to the relatively larger extent of specimen thinning around the crack tip at long crack lengths. Similar fatigue fracture behaviour has been observed in the same material under various load levels[1]. In the case of the thickest specimen there is virtually no loop area throughout the entire slow crack propagation phase. This is due to the fact that there is little or no

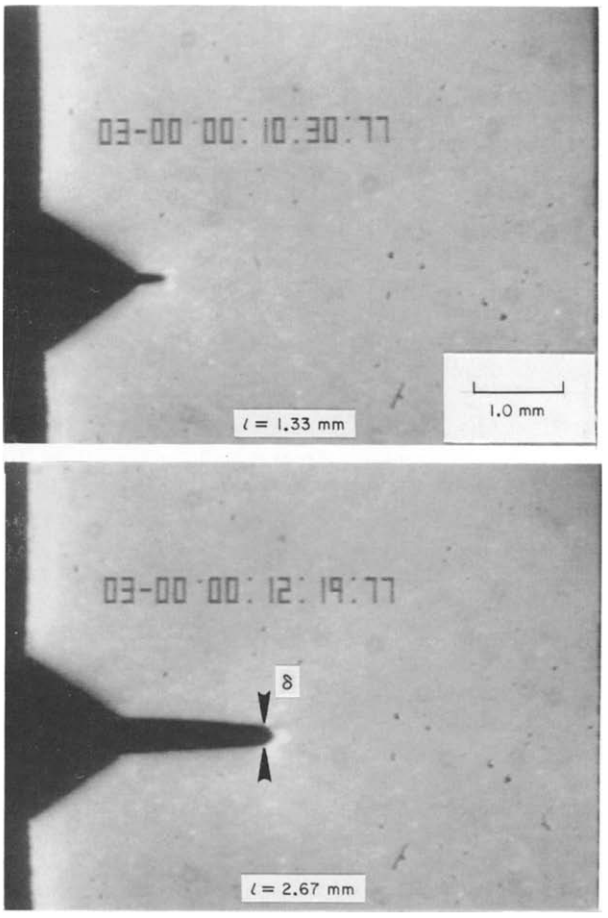

Figure 1 Typical crack opening profiles at two configurations and definition of crack tip opening displacement, δ. ($t = 5.42$ mm)

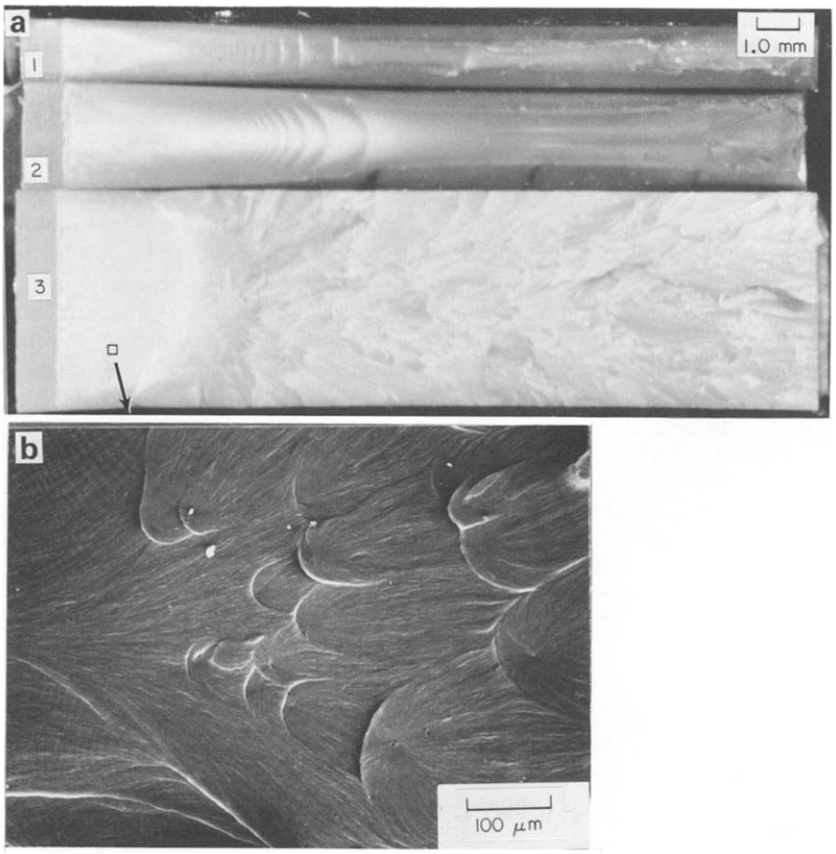

Figure 2 (a) Fracture surfaces of the three thickness study specimens: 1, t = 1.57 mm; 2, t = 2.70 mm; 3, t = 5.42 mm. Crack propagation direction is from left to right. (b) Large magnification micrograph showing striations on the fracture surface of specimen with t = 5.42 mm

lateral contraction in the thickest specimen throughout the slow crack propagation phase and is inferred from observations of fracture surfaces and of transverse sections (*Figures 2* and *5*).

Figure 2a shows an optical micrograph of the three fracture surfaces side by side. Striations are observed in the specimens with t = 1.57 mm and 2.70 mm. Although, striations cannot readily be seen in the thickest specimen, observations at greater magnification on a scanning electron microscope clearly indicate the presence of striations (*Figure 2b*). Moreover, markings bowed opposite to the crack propagation direction are seen in the brittle phase of crack growth (*Figure 2b*). These features result from coalescence of the main crack front and fronts of smaller cracks which originate from impurities ahead of the main crack tip.

In all the specimen thicknesses investigated, the striations are bowed in the direction of crack advance. In part 1 of this series of papers[1], the bowing is presumed to be due to a plane stress condition at the surface and plane strain at the middle of the specimen. In addition, different morphologies across the thickness, induced during processing, may also have contributed to the shape of the striations. Such studies, however, are beyond the scope of this paper. As in the load-level studies[1], a one-to-one correspondence is found between the cycle number and the number of bands in all three fractured specimens. Thus, the crack advances with every cycle excursion.

To examine the extent of thinning around the crack path, a specimen with t = 2.70 mm was fatigued until the crack reached a length of about 5 mm. While the specimen was kept at the maximum load, the part of the specimen around the crack path was embedded in a rapid setting epoxy. When curing was completed, the specimen was removed from the testing system. Sections normal to the crack path were then obtained by grinding and polishing procedures. Micrographs of such sections are shown in *Figure 3*. Note that fracture occurs earlier at the middle of the specimen thickness, thus resulting in the formation of a bowed striation. Furthermore, these sections suggest that damage is in the form of plastically deformed material and that lateral contraction or necking of the specimen is confined in the vicinity of the crack tip.

In part 1 of these studies[1], observations of the vicinity of the crack tip suggest the possible existence of shear bands emanating from the crack tip. Although shear bands could exist, it is also possible that the observed dark bands are due to interference between light beams reflected off the undamaged and necked regions near the crack tip (*Figure 3*). Additional experimental work is required in order to elucidate these observations.

To examine further the extent of thinning due to crack growth, transverse sections of the fractured specimens were examined under an optical microscope. Typical sections from the specimen with t = 2.70 mm are shown in *Figure 4*. For all three specimen thicknesses investigated, observations indicate that at short crack lengths lateral contraction does not occur. Thus during the early phases of fracture, cracks grow in a 'brittle' fashion. Apart from the thickest specimen, localized necking takes place around the crack tip at long crack lengths, which is associated with a 'ductile' mode of crack growth. A transverse section from the thickest specimen

is shown in *Figure 5*. Note the lack of specimen thinning and the presence of a few discontinuities underneath the main crack plane (arrow heads in *Figure 5*). It is difficult, however, to distinguish whether these discontinuities are crazes or secondary cracks. Moreover, the respective fracture profile across the specimen thickness is much more irregular than in the other fractured specimens of smaller thickness.

It should be noted that in view of the bowed crack front and the curvature of the crack surfaces at long crack lengths (*Figure 2*), values of the crack length l and crack tip opening displacement δ (*Figure 1*), measured during crack advance, are subjected to error. Whereas accurate values of l are obtained from the fracture surface as averages of a few measurements along corresponding striations, it is difficult to obtain accurate values of δ during crack growth. What is measured is a surface or plane stress value[10].

The extent of fracture surface thinning as a function

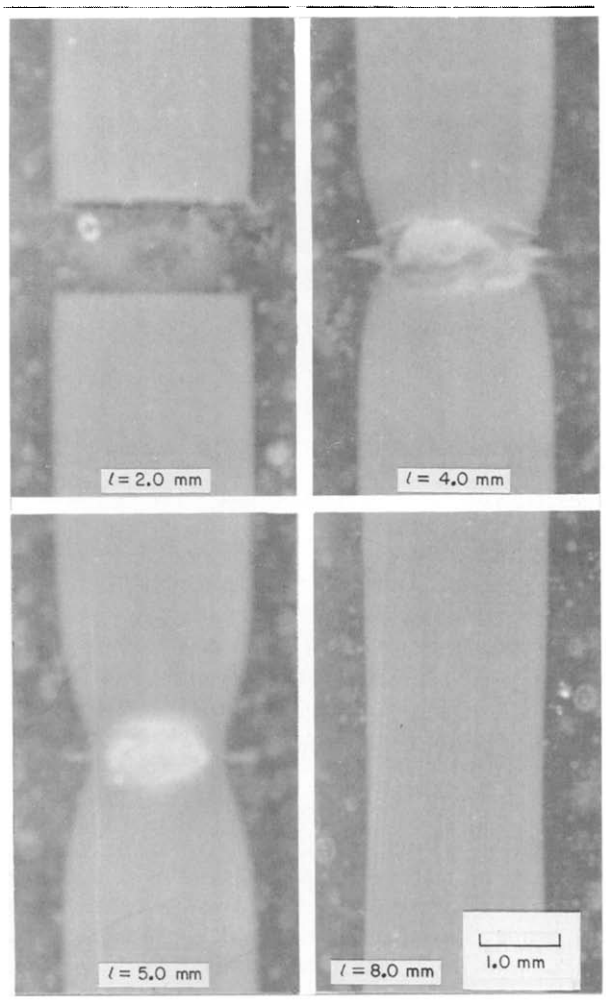

Figure 3 Transverse sections of a crack grown to a length of 5.0 mm (see text for details)

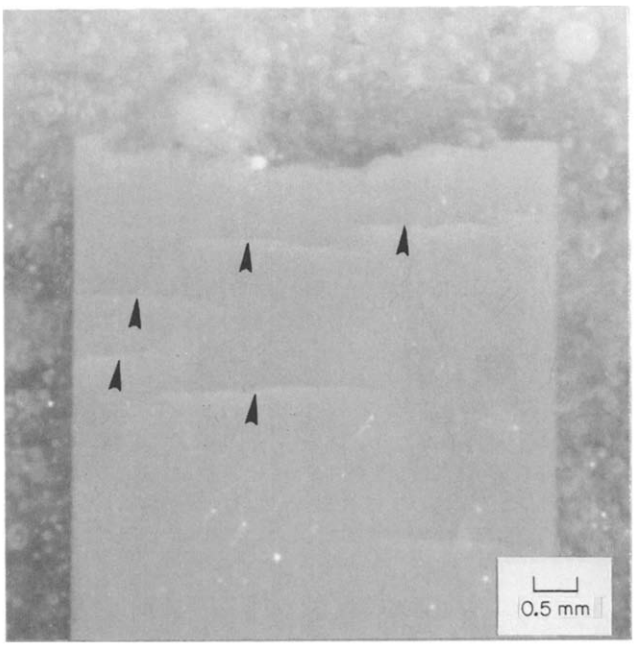

Figure 5 Transverse section of the specimen with $t = 5.42$ mm. Arrow heads indicate discontinuities

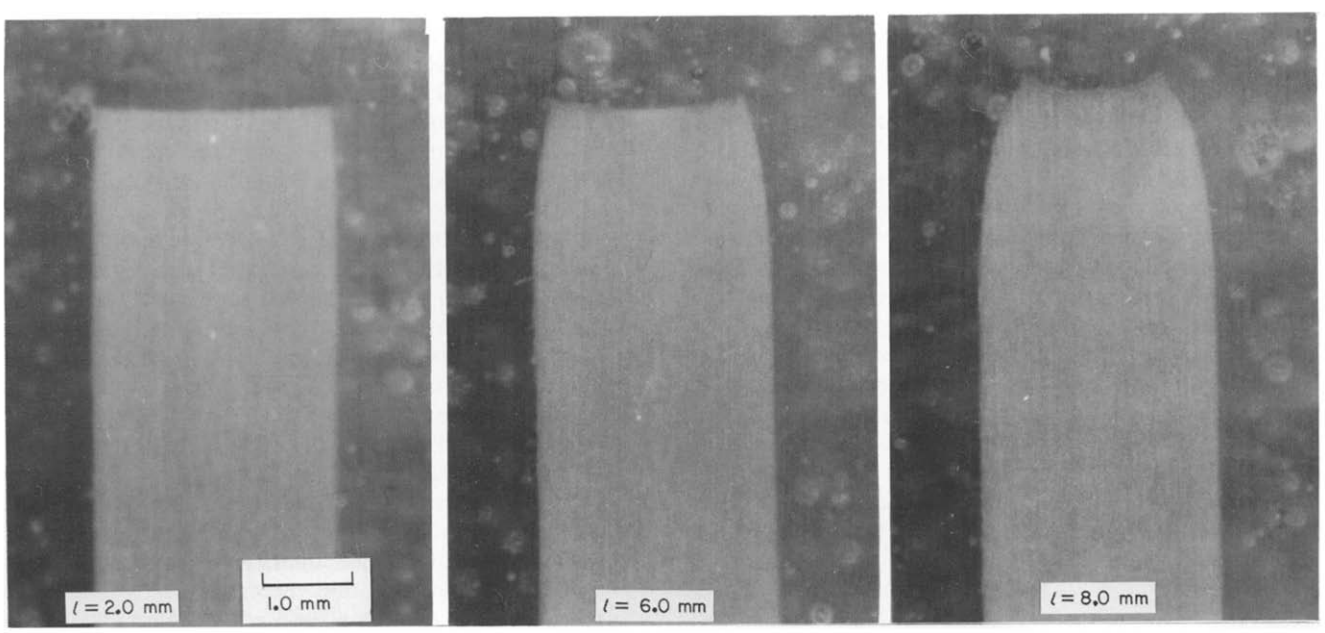

Figure 4 Typical transverse sections of a fractured specimen with $t = 2.70$ mm

of crack length for the three specimen thicknesses is shown in *Figure 6*. Since the last striation is formed after the last complete fatigue cycle is executed and the specimen fails at almost the maximum stress of the next subsequent cycle, the point of minimum thinning is taken as the critical crack length. With regard to the thickest specimen, the critical crack length is taken at the point where a sharp change in morphology of the fracture surface is observed (*Figure 2a*).

The aforementioned observations indicate that for the specimens with $t = 1.57$ and 2.70 mm, two distinct modes of fracture are observed: 'brittle' and 'ductile'. The point of 'brittle' to 'ductile' transition depends upon the thickness of the specimen. That is, as specimen thickness decreases the transition from 'brittle' to 'ductile' mode of crack growth occurs at shorter crack lengths. In the thickest specimen, 'brittle' fracture is observed throughout the slow phase of propagation.

Experimental and theoretical values of δ (equation (2)) plotted against the crack length are shown in *Figure 7*. The data suggest that during the initial phases of fatigue fracture in the specimens with $t = 1.57$ and 2.70 mm, the

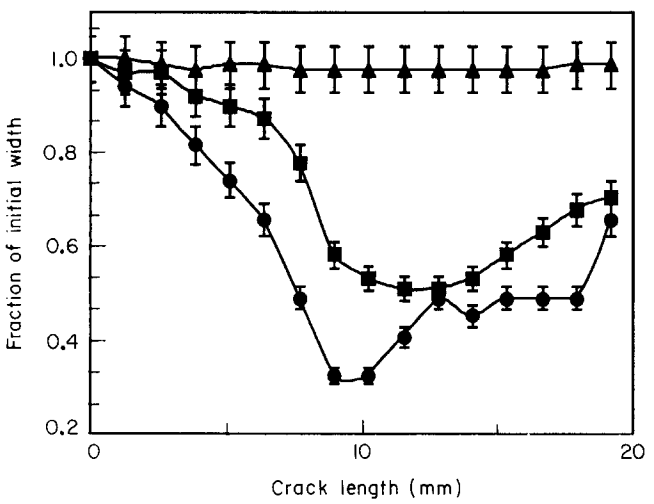

Figure 6 Extent of fracture surface thinning: ●, $t = 1.57$ mm; ■, $t = 2.70$ mm; ▲, $t = 5.42$ mm

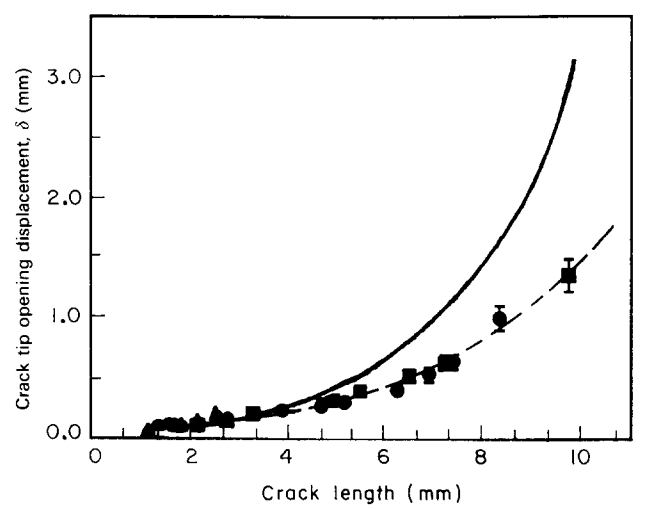

Figure 7 Crack tip opening displacement, δ, plotted against crack length: ●, $t = 1.57$ mm; ■, $t = 2.70$ mm; ▲, $t = 5.42$ mm; ——, values calculated from equation (2)

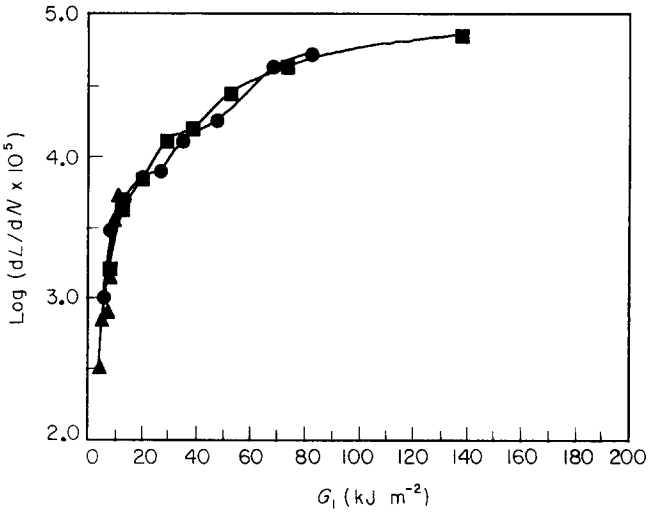

Figure 8 Crack growth kinetics as a function of G_1: ●, $t = 1.57$ mm; ■, $t = 2.70$ mm; ▲, $t = 5.42$ mm

experimental values of δ are practically equal to the calculated values. A deviation between the calculated and experimentally measured δ is manifested at crack lengths greater than about 5 mm. Although this deviation is anticipated to be due to excessive necking around the crack tip, the specimen thickness has no effect in the calculated and experimental values of δ. While it is expected that the calculated values of δ should be the same (assuming plane strain or plane stress conditions) because the applied stress is the same (equation (2)), the variation in thickness does not have any noticeable effect on the observed value of δ. A possible rationale for this behaviour is given later. When $t = 5.42$ mm, the experimental values of δ compare well with the calculated values within the entire phase of slow crack growth. This is expected since crack propagation in that specimen occurs in a 'brittle' manner (*Figure 2*).

Crack growth kinetics plotted against the elastic energy release rate, G_1, are shown in *Figure 8*. Note that for the same level of G_1, crack speed is independent of specimen thickness. Moreover, the data seemingly indicate that G_1 could be utilized to correlate crack growth kinetics for the conditions reported here.

As stated earlier, fracture in the specimen with $t = 5.42$ mm occurs in a 'brittle' manner. In the specimens with $t = 1.57$ and 2.70 mm, both modes of fracture, 'brittle' at short crack lengths and 'ductile' at long crack lengths, are observed. Thus, it is not surprising that crack speed correlates well with G_1 for the entire phase of propagation in the specimen with $t = 5.42$ mm and up to $G_1 \sim 30$ kJ for the other two specimens. Afterwards, significant irreversible deformations are developed around the crack tip in the specimens with $t = 1.57$ and 2.70 mm. Therefore, the facts that the experimental values of δ in the specimens with $t = 1.57$ and 2.70 mm are practically the same and that crack growth data are comparable for the same level of G_1, even when non-linear effects are important, suggest that the constraints around the crack tip are independent of thickness in these two specimens. Therefore, G_1 may not be an appropriate parameter to describe crack growth rates under the experimental conditions employed here. Accordingly, energy release rates evaluated from load displacement curves should be employed to correlate

fatigue crack propagation data in the ductile phase of crack growth.

Temperature effects on crack propagation mechanisms

Optical micrographs of the crack opening profiles at the maximum stress of the fatigue cycle for the temperature studies were examined to evaluate the crack opening geometries (*Figure 9*). For the experiments at environmental temperatures, T, of 39 and 50°C, the crack tip is initially round. As the crack length increases the crack tip geometry changes to a triangular shape. Unlike the crack tip angle observed in the thickness and load-level studies, the crack tip angles here are 10–15°C smaller. Moreover, the transition to a triangular crack tip shape occurs later in the crack growth process as compared to the thickness and load-level studies. On the other hand, the crack tip geometries for the specimens with $T = 63$, 75 and 100°C remain relatively round throughout the fatigue crack growth process.

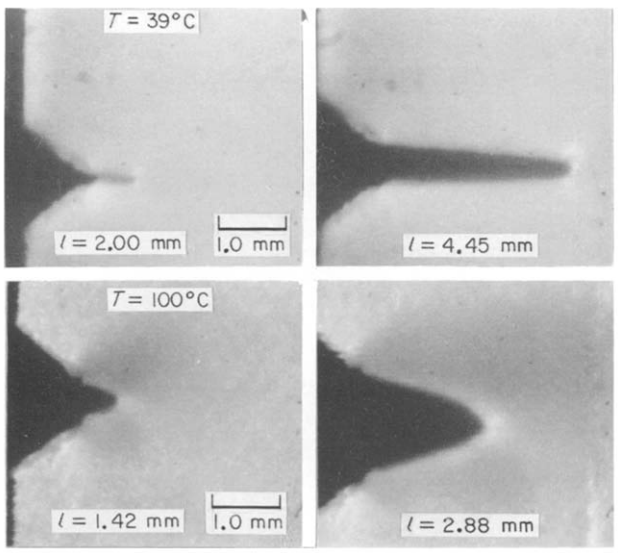

Figure 9 Typical side views of crack growth at $T = 39$ and 100°C

The evolution of the hysteresis loop for the 75°C experiment is shown in *Figure 10*. Although the hysteresis loop changes insignificantly during the initial phase of crack growth, the area of a typical loop is not negligible. This may be due to some viscoelastic effect induced at 75°C. Noticeable changes take place at long crack lengths and are attributed to the larger extent of damage in the vicinity of the crack tip.

A micrograph of the fracture surfaces of three specimens is shown in *Figure 11*. The presence of bowed striations at long crack lengths is apparent from this micrograph. Scanning electron microscopy observations verify the existence of striations at short crack lengths where they are not visible with the use of optical microscopy techniques. The appearance of striations on the fracture surface of PEEK has become a recurring event regardless of load level[1], specimen thickness or temperature.

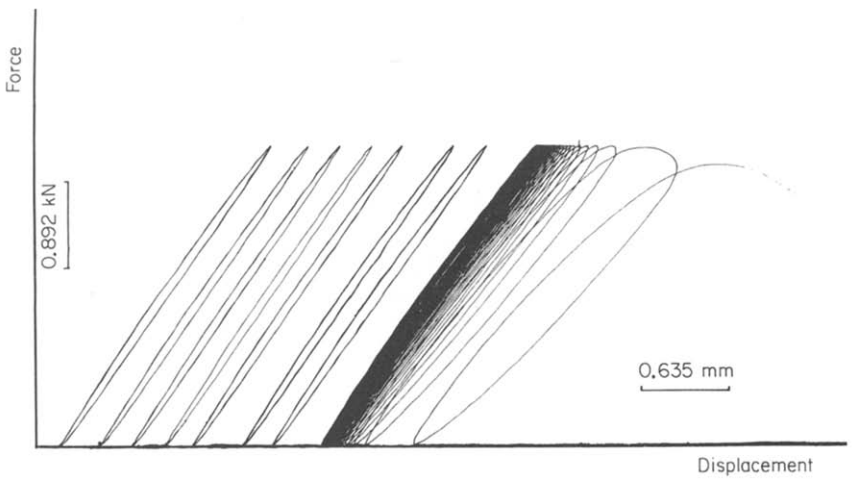

Figure 10 Evolution of hysteresis loops for $T = 75$°C

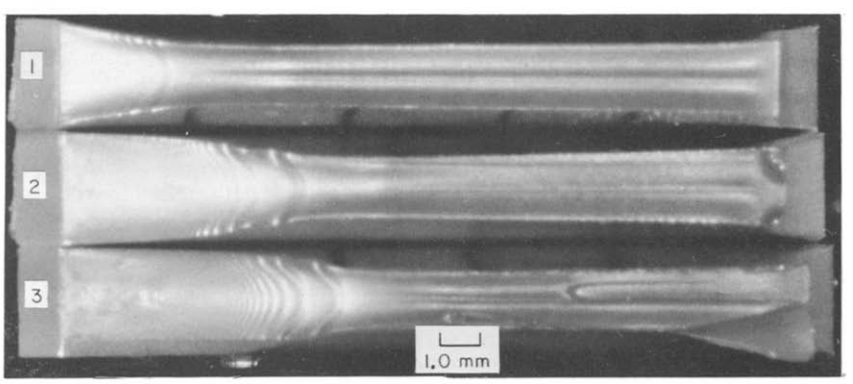

Figure 11 Fracture surfaces for specimens at three test temperatures. 1, $T = 100$°C; 2, $T = 75$°C; 3, $T = 50$°C. Crack propagation direction is from left to right

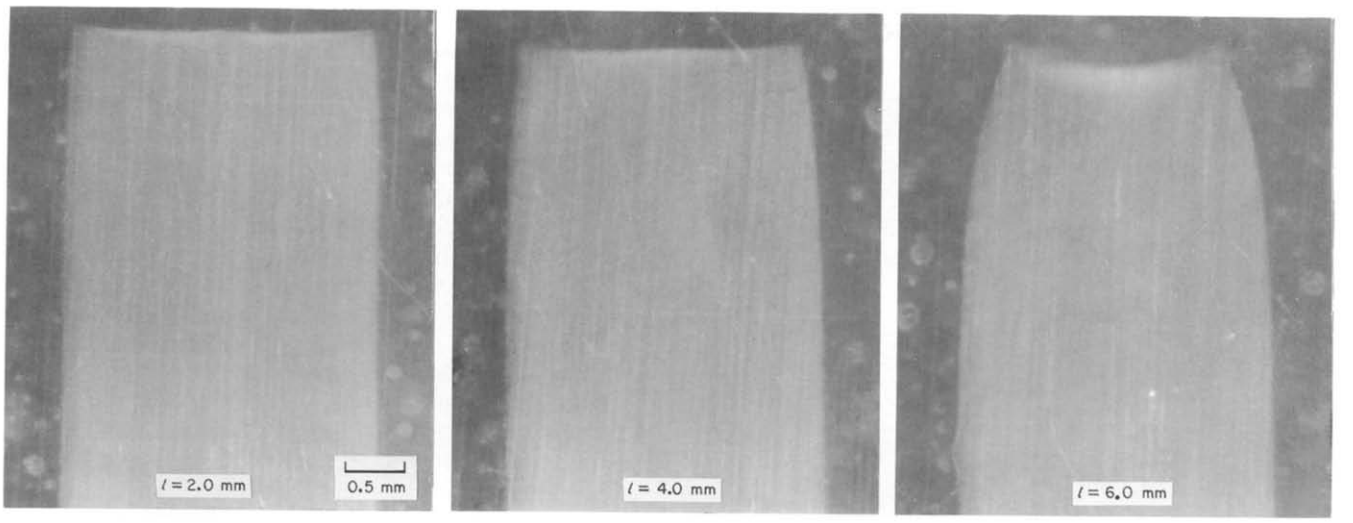

Figure 12 Typical transverse sections of a fractured specimen with $T = 75°C$

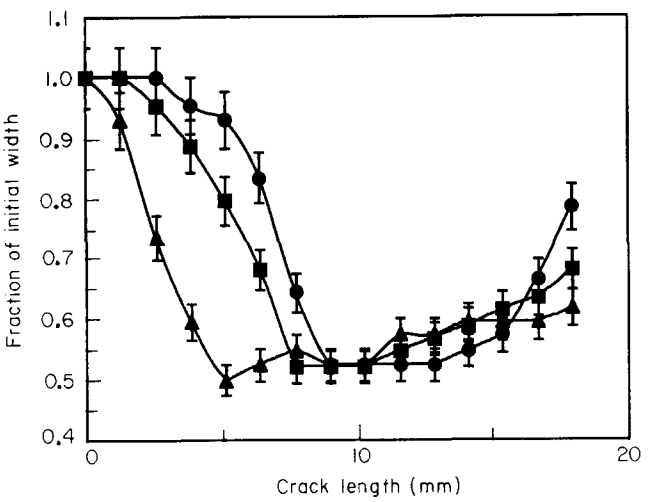

Figure 13 Extent of fracture surface thinning: ●, $T = 50°C$; ■, $T = 75°C$; ▲, $T = 100°C$

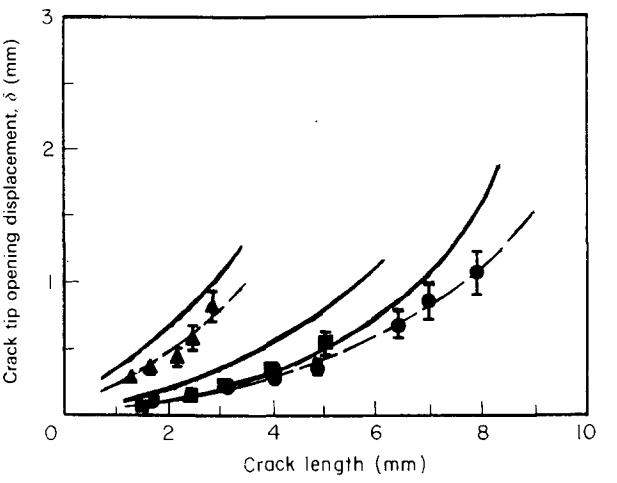

Figure 14 Crack tip opening displacement, δ, plotted against crack length: ●, $T = 50°C$; ■, $T = 75°C$; ▲, $T = 100°C$; ——, values calculated from equation (2)

Typical transverse sections of the specimen with $T = 75°C$ are shown in *Figure 12*. These observations suggest that at short crack lengths, crack propagation occurs in a 'brittle' fashion. As the crack length increases, the mode of crack growth changes to 'ductile' as indicated by the increased localized necking at the crack tip.

In *Figure 13* the extent of specimen thinning is plotted against the crack length for experiments at $T = 50$, 75 and 100°C. It appears that as the test temperature increases the crack length at which maximum thinning occurs decreases. Moreover, it is interesting to note that as the temperature increases, the extent of thinning at similar crack lengths increases (*Figure 13*). The data in *Figure 13* bring out an interesting point with respect to the rate of thinning. For the lowest temperature, thinning occurs at a relatively smooth rate until just before the maximum thinning is reached. For the intermediate temperature, the thinning occurs in a similar fashion. However, at the highest temperature, a radical drop in thickness occurs right to the point of maximum thinning.

As observed in the load-level[1] and thickness studies, it appears that there is a 'brittle' to 'ductile' transition. Observations of specimen thinning and transverse sections showing the extent of damage indicate that as the temperature increases the crack length at which the 'brittle' to 'ductile' transition occurs decreases.

Experimental and theoretical values of crack tip opening displacements δ plotted against the crack length for three temperatures are shown in *Figure 14*. In the experiment with $T = 100°C$, the values of δ evaluated with the use of equation (2) are consistently higher than the observed δ. At $T = 75°C$, a difference between the calculated and experimental values of δ appears at a crack length of about 2 mm. At $T = 50°C$, the experimental δ values are nearly equal to those evaluated from equation (2) for crack lengths up to 5 mm. At greater crack lengths the values obtained from equation (2) are greater than the experimental δ.

A plot of crack growth kinetics against the elastic energy release rate G_1 is shown in *Figure 15*. It is apparent that during the initial phases of crack growth, G_1 is a good similitude parameter for correlating fatigue crack growth kinetics at the lower temperatures examined in this study. The kinetics for $T = 100°C$ consistently deviate from the two lower temperatures throughout the stable crack growth regime.

The present studies show that when $T < 75°C$, G_1 is an appropriate parameter to use in the 'brittle' phase of

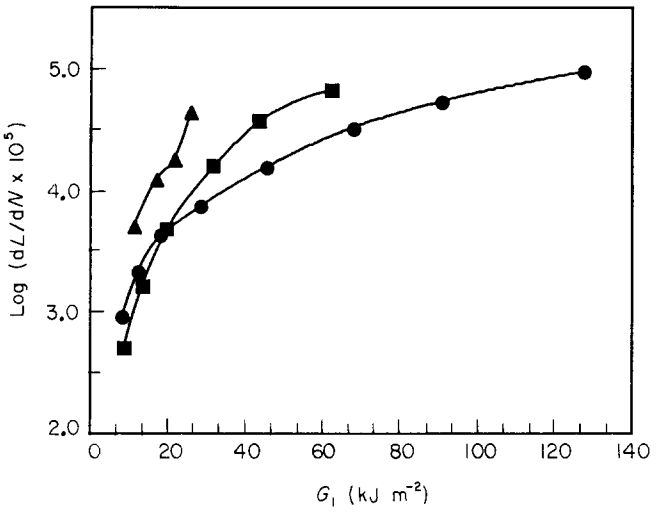

Figure 15 Crack growth kinetics as a function of G_1: ●, $T = 50°C$; ■, $T = 75°C$; ▲, $T = 100°C$

crack growth. In order to account for the ductile phase of propagation, energy release rates evaluated from load displacement curves should be available. It has been shown, however, that the actual energy release rate can be approximated by $J_1 = \sigma_y \delta^1$. Thus, J_1 could be employed to correlate fatigue crack growth rates. An attempt to describe the kinetic data with the use of a power type kinetic equation and the kinetic equation proposed by the phenomenological model of a crack layer[11], will be reported in a future publication.

CONCLUSIONS

The effects of specimen thickness and environmental temperature on fatigue crack propagation in PEEK have been reported. The results show that in all three thicknesses investigated the crack tip is initially round. The crack tip profile changes to a triangular shape with a crack tip angle of about 90°. When the specimen thickness is $t = 1.57$ or 2.70 mm, both 'brittle' and 'ductile' modes of fracture are observed. This is the result of localized necking in the vicinity of the crack tip at long crack lengths. In the experiment with $t = 5.42$ mm, crack growth occurs in a 'brittle' manner throughout the slow crack propagation phase. Damage in the form of secondary cracks (or crazes) is observed underneath the plane of the main crack, as well as relatively rough fracture surfaces. The experimental values of the crack opening displacement and the crack speed are independent of specimen thickness. In the experiments with environmental temperatures, $T = 39$ and 50°C, the crack tip geometry is initially round. Afterwards, it changes to a triangular shape with an angle of about 75°. These changes are not observed in the experiments with $T = 63$, 75 and 100°C, where the crack tip remains round throughout the fracture process. 'Brittle' and 'ductile' fractures are observed in all temperature studies. The crack opening displacements and crack growth rates increase with increase in temperature. There appears to be a critical temperature between 75 and 100°C above which the fatigue fracture behaviour of PEEK is affected.

ACKNOWLEDGEMENTS

The authors acknowledge partial financial support from the Department of Civil Engineering, Mechanics and Metallurgy at the University of Illinois, Chicago, USA. Thanks are also due to ICI, Exton, PA, USA, for providing the material.

REFERENCES

1 Brillhart, M., Gregory, B. and Botsis, J. *Polymer* 1991, **32**, 1605
2 Hertzberg, R. W. and Manson, J. A. in 'Fatigue in Engineering Plastics', Academic Press, New York,, 1980
3 Friedrich, K. and Karger-Kocsis, J. in 'Fractography and Failure Mechanisms of Polymers and Composites' (Ed. A. C. Roulin-Moloney), Elsevier, Barking, 1989, p. 437
4 Gregory, B. L. and Botsis, J. *J. Mater. Sci.* 1991, **26**, 1015
5 Tada, H., Paris, P. C. and Irwin, G. P. 'The Stress Analysis of Cracks Handbook', Del Research Corp., Helertown, Pennsylvania, 1975, p. 2.11
6 'Modern Plastics Encyclopedia', McGraw-Hill, New York, 1989, Vol. 66
7 Talbot, M. F., Springer, G. S. and Berglund, L. A. *J. Comp. Mater.* 1987, **21**, 1056
8 Burdekin, F. M. and Stone, D. E. W. *J. Stain Anal.* 1966, **1**, 145
9 Holik, A. S., Kambour, R. P., Fink, D. G. and Hobbs, S. Y. in 'Microstructural 26. Science' (Eds LeMay, Fallon and McCalls), Elsevier North Holland, 1979, Vol. 7, p. 357
10 Broek, D. in 'Elementary Fracture Mechanics', 3rd edn, Martinus Nijhoff, Dordrecht, 1982
11 Chudnovsky, A. in 'Tenth National Conference on Applied Mechanics' (Ed. J. P. Lamb), ASME, Austin, 1986, p. 97